Neurokinematic modeling of complex swimming patterns of the larval zebrafish

Scott A. Hill[a,b], Xiao-Ping Liu[c], Melissa A. Borla[c],
Jorge V. José[a,b,*], Donald M. O'Malley[a,c]

[a]*Center for Interdisciplinary Research in Complex Systems, Northeastern University, Boston MA, USA*
[b]*Department of Physics, Northeastern University, Boston MA, USA*
[c]*Department of Biology, Northeastern University, Boston MA, USA*

Abstract

Larval zebrafish exhibit a variety of complex undulatory swimming patterns. This repertoire is controlled by the 300 neurons projecting from brain into spinal cord. Understanding how descending control signals shape the output of spinal circuits, however, is nontrivial. We have therefore developed a segmental oscillator model (using *NEURON*) to investigate this system. We found that adjusting the strength of NMDA and glycinergic synapses enabled the generation of oscillation (tail-beat) frequencies over the range exhibited in different larval swim patterns. In addition, we developed a kinematic model to visualize the more complex axial bending patterns used during prey capture.
© 2004 Published by Elsevier B.V.

Keywords: Zebrafish; Swimming; Locomotion; CPG; Spinal cord

1. Introduction

The spinal cords of vertebrate animals contain segmental oscillators, or central pattern generators (CPGs), that can produce rhythmic movements. The operations

of these spinal CPGs are best understood in lower vertebrates, such as lamprey and Xenopus, where they are used for undulatory swimming [5,13,24]. Control signals descending from brainstem to spinal cord have also been studied extensively in these and other lower vertebrates, such as goldfish and zebrafish. Their lack of a corticospinal tract avoids a degree of complexity that is present in mammals. The functioning of descending control systems in higher vertebrates has been difficult to understand. Studies of lower vertebrates should reveal conserved principles by which these systems operate. The larval zebrafish takes vertebrate simplicity to an extreme: the decreased numbers of neurons allow exact identification of many cell types in both brainstem and spinal cord [1,16,17,19]; this in turn provides major experimental and modeling advantages.

One important aspect of lower vertebrate locomotion is the regulation of swimming speed, which is often correlated with the frequency of alternating left and right contractions of the axial muscles of the trunk or tail, termed tail-beat frequency (TBF). In a steady-swimming fish TBF is generally equal to the oscillation frequency of the spinal CPGs, so by understanding the modulation of CPG frequency in spinal cord we can understand a major element of the control of swim speed. In goldfish, lamprey, and other fishes, swim frequency can be modulated by stimulation of the midbrain locomotor region or bath application of NMDA; it is also known that serotonin, acetylcholine, dopamine, and other neurotransmitters influence the CPG's oscillation frequency. However, the identities and locations (in brainstem or spinal cord) of the cells involved in swim frequency control are unknown. Larval zebrafish may provide insights into this problem because they exhibit distinct swim patterns that span a broad range of tail beat frequencies, ranging from 25 to 75 Hz [6]. A critical unknown is whether or not the distinct larval swim patterns (*slow*, *burst*, and *capture*) are controlled by distinct control systems and/or specific neurotransmitters [3,21]. Modeling the different types of swimming behavior using a combined neural and kinematic model can shed light onto the presence and relevance of different motor control elements.

The functioning of spinal networks that underlie locomotion in fishes and tadpoles has been extensively modeled (see e.g. [7,8,13,23]). We created a zebrafish neural model, based on previous Xenopus spinal network models, of the CPGs in the larval zebrafish spinal cord, incorporating known properties of the oscillators underlying swimming [25]. The spinal interneuron types in zebrafish [14] are likely homologous to those in both Xenopus and lamprey [10]. We explored the control of TBF, and found that by altering the strengths of AMPA, NMDA and glycinergic-like synapses (all known to be present in lower vertebrate spinal cords), we were able to generate TBFs that spanned the range of speeds observed during burst and slow swimming behaviors. We also created a simple mechanical or "kinematic" model (that can be driven by the neural model) to visualize how the spinal neural activity might be transformed into larval behaviors. Our ultimate goal in creating this neurokinematic model is to introduce a tool for testing theories of descending motor control in the larval zebrafish.

2. Methods

Fig. 1 shows the structure of our neural model, which is a simplification of the larval spinal circuitry [14] incorporating the minimal elements required to generate rhythmic, propagating alternating activity. Each segmental oscillator consists of two neurons, with NMDA and AMPA-like autosynapses, which are connected by glycinergic synapses. An oscillator can be triggered with a single excitatory pulse to one cell, followed by a single pulse to the other cell several milliseconds later (7 ms in our simulations). Individual oscillators are connected into a 25-segment chain (corresponding to the approximately 25 segments in the zebrafish spinal cord), with nearest-neighbor descending excitatory synaptic connections; the entire chain can be started merely by triggering the head segment.

We use cells with the standard Hodgkin–Huxley channels provided by the *NEURON* software package: persistent potassium ($\bar{g}_K = 0.036\,\text{S/cm}^2$, $E_K = -77\,\text{mV}$), transient sodium ($\bar{g}_{Na} = 0.12\,\text{S/cm}^2$, $E_{Na} = 50\,\text{mV}$), and leak ($g_L = 0.0003\,\text{S/cm}^2$, $E_L = -54.3\,\text{mV}$) channels. Our synapses are modeled using the difference of two exponentials, with rise time $\tau_1 (= 1\,\text{ms})$ and fall time τ_2. See [9, p. 182] for details. The three types of synapses we used were AMPA ($\tau_2 = 6\,\text{ms}$, $E = 0\,\text{mV}$), NMDA ($\tau_2 = 80\,\text{ms}$, $E = 60\,\text{mV}$), and glycine ($\tau_2 = 2\,\text{ms}$, $E = -80\,\text{mV}$).

Our kinematic model is meant to translate the neural signals from the spinal circuitry into observable kinematic behaviors. To do so, we use a relatively simple transformation of putative neural output into effects on the radius of curvature of a line segment representing the trunk of the larva. This model does not take into account the full physics (e.g., elasticity and hydrodynamics) of the situation; nevertheless, it does approximate the observed axial kinematics recorded experimentally with a high-speed camera.

Suppose that each segment x is receiving a neural signal $F_s(x, t)$ at time t from the spinal circuitry: $F_s > 0$ for a signal to the right side of the segment, $F_s < 0$ for a signal to the left. We suppose that this signal is integrated through exponential synapses, so
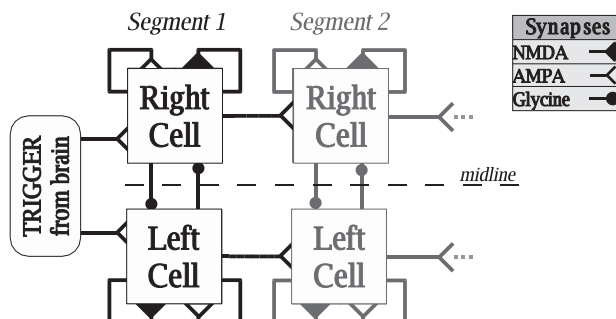

Fig. 1. Schematic diagram of the neural oscillator model. The squares represent neurons, and each line indicates one of three types of synaptic connection: glycinergic (fast inhibitory), AMPA-like (fast excitatory), or NMDA-like (slow excitatory). Only the first two segments of a 25-segment chain are shown.

that the signal passing to the muscles is

$$F_{\mathrm{m}}(x,t) = \int_{-\infty}^{t} F_{\mathrm{s}}(x,t')[\mathrm{e}^{(t'-t)/\tau_2} - \mathrm{e}^{(t'-t)/\tau_1}]\,\mathrm{d}t', \tag{1}$$

where τ_1 and τ_2 are the growth and decay time constants of the synapse (we use $\tau_1 = 6\,\mathrm{ms}$ and $\tau_2 = 8\,\mathrm{ms}$ in our calculations.) Assuming that the muscle contracts linearly as a function of F_{m}, it follows that the radius of curvature of segment x is

$$R(x,t) = W(x)/F_{\mathrm{m}}(x,t). \tag{2}$$

$W(x)$ is a function describing the stiffness, or resistance to bending, of segment x. It takes into account the width of the body (the tail is more flexible, and bends more than the rostral trunk).

We can feed the output of our neural model directly into this system, but it is also useful to introduce a (more) artificial signal. We build this signal out of three components: an oscillatory signal $F_{\mathrm{osc}}(x,t)$, which is a series of delta functions propagating caudally; a bending signal F_{bend}, which is a tonic signal applied to one side of all segments at once; and a rostral stiffening signal, which reduces the signal to the first x_{inh} rostral segments by a factor f_{inh}. The first two components are responsible for swimming and turning, respectively. The stiffening signal is seen in larvae during prey capture, where the fish keeps its head relatively still while adjusting its orientation with its tail. We can write our artificial neural signal as

$$F_{\mathrm{s}}(x,t) = (F_{\mathrm{osc}}(x,t) + f_{\mathrm{bend}}) \times \begin{cases} f_{\mathrm{inh}}, & x \leqslant x_{\mathrm{inh}}, \\ 1, & x > x_{\mathrm{inh}}, \end{cases} \tag{3}$$

where f_{bend} is a constant and

$$F_{\mathrm{osc}}(x,t) = f_{\mathrm{osc}} \begin{cases} 1, & x \equiv 2\pi v t \ (\mathrm{mod}\,\lambda), \\ -1, & x \equiv 2\pi v t + \lambda/2 \ (\mathrm{mod}\,\lambda), \\ 0, & \text{otherwise.} \end{cases} \tag{4}$$

The parameter v is the TBF, and λ is the length (in number of segments) of the resulting wave which propagates down the fish.

3. Results and discussion

We began by studying a single segment of the neural model shown in Fig. 1. A transient trigger pulse to this model initiates sustained alternating activity, mimicking Xenopus spinal cord, where a transient stimulus produces a sustained bout of swimming [23]. The first larval-zebrafish specific task was to generate the range of TBFs used in different swimming behaviors. The frequency of oscillation was calculated on a half-cycle basis (termed "instantaneous" TBF in [3]). Fig. 2 shows how instantaneous TBF varies with time, with each trace representing the frequency profile for a specific value of the NMDA synaptic conductance. In all cases, there is an initial transient period, 15 to 20 cycles long, where the TBF
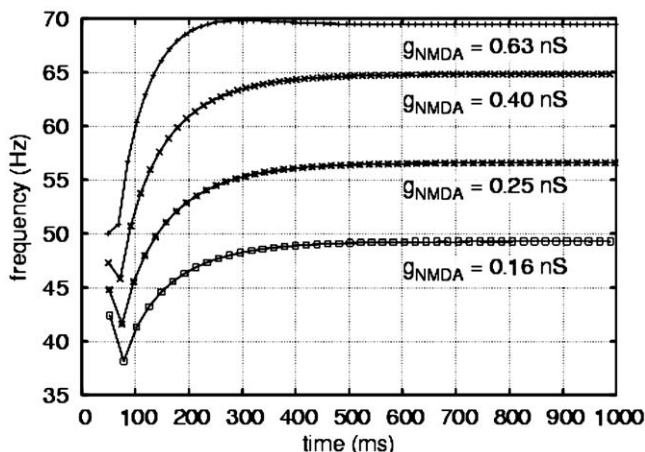
Fig. 2. Instantaneous TBF in a single segmental oscillator, for several values of g_{NMDA}. Each point represents the iTBF for the left neuron; the corresponding points from the right side gives near-identical results. Oscillators approach a steady-state frequency only after an initial "wind-up" period.
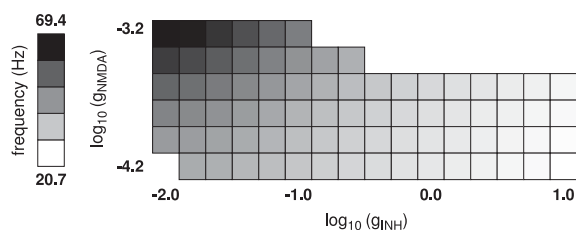

Fig. 3. A density plot showing the steady-state frequency of a single oscillator as we modify the synaptic conductances g_{NMDA} and g_{INH}, fixing $g_{AMPA} = 10^{-4}$. All conductances are in μS, and all frequencies are in Hz. The missing regions in the upper-right and lower-left corners represent nonoscillatory states.

increases by about a third before settling into an indefinite steady state with constant frequency. We subsequently re-inspected behavioral sequences, and found varying degrees of wind-up in some, but not all, experimentally recorded swim bouts [3]. It is unknown whether the biological and simulational wind-up behaviors are related, but the phenomenon lasts much longer in the model than in the lab.

To evaluate the range of oscillator or TBFs that might be generated with this simple model, we tested different combinations of synaptic strengths (conductances). Varying the strengths of the NMDA and glycinergic synapses was found to alter the steady-state oscillator frequency (Fig. 3): increasing the NMDA conductance increased TBF, whereas increasing the glycinergic conductance decreased it. The AMPA conductance can also affect TBF, but to a lesser extent. Different combinations of conductances could give rise to the entire range of TBFs observed in different larval swim patterns, from the slow swim (25–40 Hz) to burst swim (45–75 Hz; [6]). This is just one potential means of varying oscillator frequency (or TBF), implemented in a reduced system (i.e. a two-cell model), but it illustrates how

a minimal model of larval zebrafish spinal cord, with just a few essential conductances, can give rise to a range of outputs relevant to the larval behaviors. In this model, each crossed inhibitory signal results in one post-inhibitory rebound firing of a single action potential, but to more completely capture slow and burst swims we will need to incorporate mechanisms that regulate the strength of output of the motoneuron pools.

We next extended the model to a 25-segment chain of oscillators, creating a kind of artificial spinal cord that should facilitate quantitative analyses of the influences of descending signals on spinal network activity. The firing pattern of the model spinal cord is illustrated in Fig. 4. The firing of segment number 1 shows an alternating left-right pattern over the duration of the simulation. In successively more caudal segments, the firing is delayed, matching the general pattern of undulatory swimming. As in the single-segment model, each segment along the chain showed a frequency wind-up period. In this model a fixed intersegmental time-delay (nominally a synaptic delay) was used to establish the phase relationship between segments, but a more realistic model might include ascending and descending connections of varying strengths and lengths, as in lamprey [8,18].

The kinematic model of the larval trunk is a complementary tool for exploring theories of descending motor control. Preliminary work [15] assumed that the fish was equally flexible from trunk to tail ($W(x) = 1$ in Eq. (2)), with partial success. By accounting for the increased flexibility of the tail (e.g. by making $W(x)$ linear), however, we can better simulate the trunk kinematics observed during slow swims and J-turns (Fig. 5). J-turns are unique locomotive maneuvers that contribute to the larval prey-capture behavior [2]. They require repetitive, asymmetric and far-caudal contractions of axial musculature. This might in principle be achieved by sending an
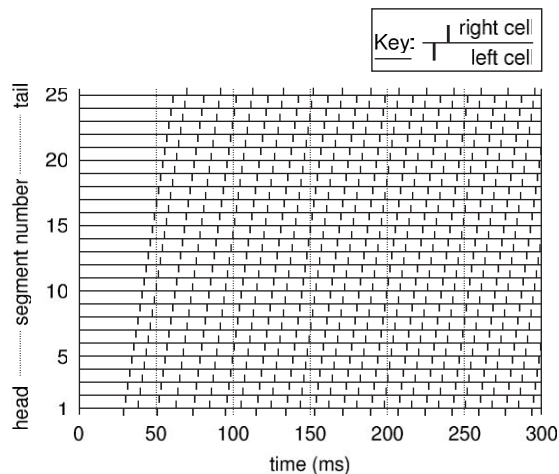

Fig. 4. Rastergram for a chain of 25 segmental oscillators. Each horizontal line corresponds to a single oscillator; ticks drawn below each line are for action potentials on the left, and above for those on the right. Parameters: $g_{AMPA} = 10^{-4}\,\mu S$, $g_{NMDA} = 6 \times 10^{-4}\,\mu S$, $g_{INH} = 10^{-2}\,\mu S$, $g_{descending} = 10^{-2}\,\mu S$.
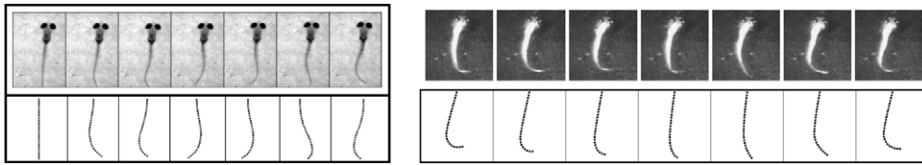
Fig. 5. Comparison of a 7-day old larval zebrafish with our kinematic model during a slow swim (left) and a J-turn (right).

asymmetric excitatory brainstem signal exclusively to far-caudal spinal cord; however, a survey of the spinal outputs of zebrafish reticulospinal neurons revealed no neurons with the requisite arborization pattern [11]. Alternatively, neurons that selectively arborize in rostral spinal cord (which were observed) might be activated bilaterally to stiffen the rostral musculature. In conjunction with such signals, other neurons that arborize along the entire length of spinal cord could then generate far-caudal contraction. In our model, this is implemented as a bilateral "inhibitory" rostral signal, but this is kinematically equivalent to stiffening the rostral end of the larva by bilateral excitation of rostral motoneurons.

4. Future directions

As we extend the neural model's capabilities to produce dynamically varying bend amplitudes, we hope to produce an increasingly realistic "artificial spinal cord" that can be used to test ideas of how the larval locomotive repertoire is generated. The kinematic model is useful here because it provides a first approximation of how complex neural model outputs might affect axial kinematics. Further extensions of this model should incorporate known constraints of the larval CNS, such as the diversity of brainstem and spinal systems involved in swimming and turning behaviors [14,20,22], and the wide distribution of activity during escape behaviors [4,12]. By incorporating such constraints, the combined neurokinematic model should become increasingly useful in generating experimentally testable hypotheses of descending and spinal control of vertebrate locomotion.

References

[1] R.R. Bernhardt, A.B. Chitnis, L. Lindamer, J.Y. Kuwada, Identification of spinal neurons in the embryonic and larval zebrafish, J. Comput. Neurol. 302 (1990) 603–616.

[2] M.A. Borla, D.M. O'Malley, High-speed imaging of tracking swims used in the larval zebrafish prey capture behavior, Soc. Neurosci. Abstr. 28 (2002) 361.18.

[3] M.A. Borla, B. Palecek, S.A. Budick, D.M. O'Malley, Prey capture by larval zebrafish: evidence for fine axial motor control, Brain Behav. Evol. 60 (2002) 207–229.

[4] T.J. Bosch, S. Maslam, B.L. Roberts, Fos-like immunohistochemical identification of neurons active during the startle response of the rainbow trout, J. Comput. Neurol. 439 (2001) 306–314.

[5] J.T. Buchanan, Contributions of identifiable neurons and neuron classes to lamprey vertebrate neurobiology, Prog. Neurobiol. 63 (1999) 441–466.

[6] S.A. Budick, D.M. O'Malley, Locomotive repertoire of the larval zebrafish: swimming, turning, and prey capture, J. Exp. Biol. 203 (2000) 2565–2579.

[7] N. Dale, Experimentally derived model for the locomotor pattern generator in the Xenopus embryo, J. Physiol. 489.2 (1995) 489–510.

[8] N. Dale, Coordinated motor activity in simulated spinal networks emerges from simple biologically plausible rules of connectivity, J. Comput. Neurosci. 14 (2003) 55–70.

[9] P. Dayan, L.F. Abbott, Theoretical Neuroscience, MIT Press, Cambridge, MA, 2001.

[10] J.R. Fetcho, The spinal motor system in early vertebrates and some of its evolutionary changes, Brain Behav. Evol. 40 (1992) 82–97.

[11] E. Gahtan, D.M. O'Malley, Visually-guided injection of identified reticulospinal neurons in zebrafish, J. Comput. Neurol. 459 (2003) 186–200.

[12] E. Gahtan, N. Sankrithi, J.B. Campos, D.M. O'Malley, Evidence for a widespread brainstem escape network in larval zebrafish, J. Neurophysiol. 87 (2002) 608–614.

[13] S. Grillner, The motor infrastructure, from ion channels to neuronal networks, Nat. Rev. Neurosci. 4 (2003) 573–586.

[14] M.E. Hale, D.A. Ritter, J.R. Fetcho, A confocal study of spinal interneurons in living larval zebrafish, J. Comput. Neurol. 437 (2001) 1–16.

[15] S.A. Hill, M.A. Borla, J.V. José, D.M. O'Malley, Modeling the neural control of zebrafish locomotive behaviors, Soc. Neurosci. Abstr. 29 (2003) 278.10.

[16] C.B. Kimmel, S.L. Powell, W.K. Metcalfe, Brain neurons which project to the spinal cord in young larvae of the zebrafish, J. Comput. Neurol. 205 (1982) 112–127.

[17] C.B. Kimmel, W.K. Metcalfe, E. Schabtach, T-reticular interneurons, a class of serially repeating cells in the zebrafish hindbrain, J. Comput. Neurol. 233 (1985) 365–376.

[18] J.H. Kotaleski, S. Grillner, A. Lansner, Neural mechanisms potentially contributing to the intersegmental phase lag in lamprey: I. Segmental oscillations dependent on reciprocal inhibition, Biol. Cybern. 81 (1999) 317–330.

[19] D.W. Liu, M. Westerfield, Function of identified motoneurons and coordination of primary and secondary motor systems during zebrafish swimming, J. Physiol. 403 (1988) 73–89.

[20] D.M. O'Malley, Y.-H. Kao, J.R. Fetcho, Imaging the functional organization of zebrafish hindbrain segments, Neuron 17 (1996) 1145–1155.

[21] D.M. O'Malley, Q. Zhou, E. Gahtan, Probing neural circuits in the zebrafish: a suite of optical techniques, Methods 30 (2003) 49–63.

[22] D.A. Ritter, D.H. Bhatt, J.R. Fetcho, In vivo imaging of zebrafish reveals difference in the spinal networks for escape and swimming movements, J. Neurosci. 21 (2001) 8956–8965.

[23] A. Roberts, M.J. Tunstall, Mutual re-excitation with post-inhibitory rebound: a simulation study on the mechanisms for locomotor rhythm generation in the spinal cord of Xenopus embryos, Eur. J. Neurosci. 2 (1990) 11–23.

[24] A. Roberts, S.R. Soffe, E.S. Wolf, M. Yoshida, F.-Y. Zhao, Central circuits controlling locomotion in young frog tadpoles, Ann. NY Acad. Sci. 860 (1998) 19–34.

[25] M.J. Tunstall, A. Roberts, S.R. Soffe, Modelling inter-segmental coordination of neuronal oscillators: synaptic mechanisms for uni-directional coupling during swimming in Xenopus tadpoles, J. Comput. Neurosci. 13 (2002) 143–158.